

## Spin-Dependent Acoustic Response in the Nonunitary $A_1$ and $A_2$ Phases of Superfluid $^3\text{He}$ under High Magnetic Fields

S. Murakawa,<sup>1,\*</sup> A. Yamaguchi,<sup>2,†</sup> M. Arai,<sup>1</sup> M. Wasai,<sup>1</sup> Y. Aoki,<sup>2,‡</sup> H. Ishimoto,<sup>2</sup> R. Nomura,<sup>1</sup> Y. Okuda,<sup>1</sup> Y. Nagato,<sup>3</sup> S. Higashitani,<sup>3</sup> and K. Nagai<sup>3</sup>

<sup>1</sup>*Department of Physics, Tokyo Institute of Technology, Tokyo 152-8551, Japan*

<sup>2</sup>*Institute for Solid State Physics, University of Tokyo, Chiba 277-8581, Japan*

<sup>3</sup>*Graduate School of Integrated Arts and Sciences, Hiroshima University, Hiroshima 739-8521, Japan*

(Received 14 October 2014; published 10 March 2015)

The transverse acoustic impedance of superfluid  $^3\text{He}$  was measured in the  $A_1$  and  $A_2$  phases up to 13 T to investigate the surface states in nonunitary superfluids. The temperature dependence of the impedance was much larger in the  $A_1$  phase than in the  $A_2$  phase. This nonsymmetric behavior indicates that momentum exchange with walls for spin-down surface states is quite different from that for spin-up surface states. The spin-dependent response might be a reflection of an essential feature of the nonunitary states where gap amplitudes depend on spin states. Weak-coupling theories ignore any spin-dependent processes and do not account for the nonsymmetric behavior.

DOI: 10.1103/PhysRevLett.114.105304

PACS numbers: 67.30.hp, 43.58.Bh, 67.30.ep, 74.45.+c

In general, surface scattering has a significant effect on the local quasiparticle states of unconventional superfluids and superconductors, which are fermionic condensates with nonzero angular momentum of Cooper pairs [1–4]. Depending on the characteristics of the condensates and the surface boundary conditions, various kinds of surface states form near the surface. For example, surface Andreev bound states (SABS) appear in the vicinity of the surface of unconventional superfluids and superconductors when the order parameter changes its sign via reflection, regardless of whether they are topological or nontopological. In the case of topological superfluids and superconductors, most of which exist in spin triplet states, quasiparticles in the bound states have the properties of Majorana fermions formed by a bulk-edge (surface) correspondence [5–7]. Even in nontopological superfluids with no sign change via reflection, such as the  $^3\text{He}$   $A$  phase, diffusive scattering on rough walls induces the formation of surface states [8,9]. Since surface states have received increasing attention in recent research, it is urgent to classify them and elucidate their physical properties. We measured the transverse acoustic impedance of the nonunitary  $A_1$  and  $A_2$  phases of superfluid  $^3\text{He}$  and found that the transverse response of the surface states was highly spin dependent.

Because spin-triplet  $p$ -wave superfluid  $^3\text{He}$  has internal degrees of freedom, superfluid  $^3\text{He}$  has multiple phases [10,11]. Without a magnetic field, there exist two phases: the  $A$  and  $B$  phases. The  $A$  phase is an equal spin pairing state in which pairs are formed of the same spin states, i.e.,  $|\uparrow\uparrow\rangle$  and  $|\downarrow\downarrow\rangle$ . Under a magnetic field, the  $A$  phase stabilizes over a wider pressure and temperature region and a different phase appears near superfluid transition temperature  $T_c$ . This phase is called the  $A_1$  phase and the transition temperature  $T_{c1}$  is higher than  $T_c$  in zero magnetic field

[10–12]. The  $A_1$  phase is another equal spin pairing state and its superfluid component consists of just one set of paired spin condensates  $|\uparrow\uparrow\rangle$ , where the magnetic field is applied downwards. Thus, only the order parameter  $\Delta_{\uparrow\uparrow}$  grows below  $T_{c1}$ , while  $\Delta_{\downarrow\downarrow}$  is zero. Below a certain temperature  $T_{c2}$ , another paired spin condensate  $|\downarrow\downarrow\rangle$  grows and  $\Delta_{\downarrow\downarrow}$  begins to develop. This spin polarized  $A$  phase is known as the  $A_2$  phase. The  $A_1$  and  $A_2$  phases are a rare established example of nonunitary superfluid states in which spin-up and spin-down Cooper pairs have different gap amplitudes. While nonunitary phases have been proposed for several heavy fermion superconductors [13], the superfluid  $A_1$  and  $A_2$  phases provide a good testing ground for studying the surface states of nonunitary states.

Let us review the surface states of the  $A$  phase on a rough (diffusive) wall. At a distance from the wall that is similar to the coherence length, incoherent phase mixing during the diffusive scattering leads to the suppression of the order parameter. A different type of surface state from SABS forms there near the Fermi energy; the surface density of states (SDOS) becomes flat and gapless [8,9,14]. The surface states have a similar formation mechanism to SABS in the sense that destructive interference via scattering is essential in systems with internal degrees of freedom. However, they are not exactly the same as SABS, which can form even on specular surfaces. In the  $A_1$  and  $A_2$  phases, each spin component has a similar surface state structure as the  $A$  phase when their energies are scaled by the corresponding gap energies  $\Delta_{\uparrow\uparrow}$  and  $\Delta_{\downarrow\downarrow}$ , respectively.

We performed complex transverse acoustic impedance  $Z$  measurements [15] that have been demonstrated to be very sensitive to the surface states in both the  $A$  and  $B$  phases [9,16], because low energy surface states play a major role in the exchange of transverse momentum between a wall

and superfluid  $^3\text{He}$ . This provides spectroscopic information on the surface states when the acoustic energy  $\hbar\omega$  is comparable to the superfluid gap energy. The recent  $Z$  measurement in the superfluid  $B$  phase clarified that the energy dispersion of SABS exhibits a distinct linear dependence on momentum, forming the so-called Majorana cone in the specular limit [7,17–19].

$Z$  is defined as the ratio of the stress tensor  $\Pi$  of the liquid on a wall to the wall velocity  $u$ ,  $Z = \Pi/u$ . We used an AC-cut quartz transducer, which oscillated transversely, immersed in liquid  $^3\text{He}$  to measure  $Z$ . The transducer was installed in the cell 0.5 mm away from the cell wall. The surface of the transducer was gold plated to make a coaxial electrode. The resonance frequency  $f(= \omega/2\pi)$  and the  $Q$  factor of the transducer were measured using the continuous wave bridge method [15,16]. The real and imaginary components of  $Z$  were obtained separately as  $Z = Z' + iZ'' = (\frac{1}{4}m\pi Z_q \Delta Q^{-1}) + i(\frac{1}{2}m\pi Z_q \Delta f/f)$ , where  $Z_q$  is the acoustic impedance of the quartz and  $m$  is the harmonic number of the transducer [10].  $\Delta f$  and  $\Delta Q^{-1}$  are changes from the high temperature limit. The fundamental resonance frequency of the transducer was 9.42 MHz, but the higher harmonics  $m = 3, 5,$  and  $7$  were also used.

The experimental cell was cooled by a nuclear demagnetization refrigerator. We were able to apply a magnetic field to the cell separately using another superconducting magnet. The direction of the magnetic field was perpendicular to the transducer surface. The temperature was measured by a calibrated  $^3\text{He}$  melting curve thermometer located in a low magnetic field region and in good thermal contact with the liquid. A vibrating wire thermometer placed in the liquid  $^3\text{He}$  acted as a marker [20] for  $T_{c1}$  and  $T_{c2}$  and was used as a secondary thermometer. The experiments were carried out in a static magnetic field of up to 13 T and liquid pressures between 1.2 and 3.3 MPa.

Figure 1 shows the temperature dependence of  $Z'$  and  $Z''$  at several frequencies. The pressure and magnetic field were  $P = 2.1$  MPa and  $B = 5.0$  T. With these parameters,  $T_{c1}$  is 2.41 and  $T_{c2}$  is 2.17 mK, so the ratio  $T_{c2}/T_{c1}$  is 0.90, which is shown by the vertical solid line in Fig. 1 [21,22]. Here,  $Z_0$  is the normal liquid value of  $Z$  just above  $T_{c1}$  and the vertical axis is the normalized deviation from  $Z_0$ . We examine the temperature dependence from the high temperature side in the  $A_1$  phase. At the lowest frequency, 9.42 MHz,  $Z'$  had a peak at a temperature slightly lower than  $T_{c1}$ . The peak became broader and shifted to lower temperatures at higher frequencies.  $Z''$  steeply decreased with a clear kink just below  $T_{c1}$  at the lowest frequency. The temperatures where the kink appeared are indicated by arrows; they also shifted to lower temperature at higher frequencies.  $Z''$  saturated at frequency-dependent values at lower temperatures. This characteristic temperature dependence in the  $A_1$  phase was very similar to that observed in the  $A$  phase with no magnetic field [9,23]. To obtain the energy scale that characterizes the kink temperatures, we

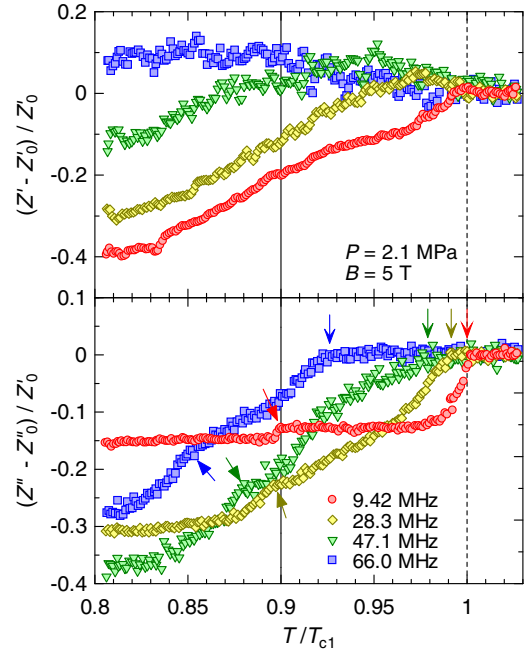


FIG. 1 (color online). Temperature dependence of the real  $Z'$  and imaginary  $Z''$  components of the transverse acoustic impedance for various frequencies at 2.1 MPa and 5 T. Changes from the normal states value  $Z_0$  just above  $T_{c1}$  are plotted. The vertical dotted line corresponds to  $T_{c1}$  and the vertical solid line corresponds to  $T_{c2}$ . The arrows indicate the kink temperatures, below which  $Z''$  started to decrease with cooling. The temperature dependence of  $Z''$  in the  $A_2$  phase was smaller than that in the  $A_1$  phase.

compared  $\Delta_{\uparrow\uparrow}$  at the kink temperatures with the acoustic energies and found that they had the nearly frequency-independent values of  $\Delta_{\uparrow\uparrow}/\hbar\omega = 0.63 \pm 0.07$ .

In the  $A_2$  phase, the kink was also observed for  $Z''$  at the temperatures indicated by the arrows in Fig. 1. The kink appeared just below  $T_{c2}$  at the lowest frequency and shifted to lower temperatures at higher frequencies. The broad peak of  $Z'$  was obscured in the  $A_2$  phase such that no clear features were recognizable; this is possibly because the peak was buried in noise due to the background temperature dependence of the spin-up component continuing from the  $A_1$  phase. In the  $A_2$  phase at the kink temperatures, we also compared  $\Delta_{\downarrow\downarrow}$  with the acoustic energies and found  $\Delta_{\downarrow\downarrow}/\hbar\omega = 0.61 \pm 0.03$ ; this value was nearly frequency independent and was almost the same as that in the  $A_1$  phase. This fact supports a common belief that the gap amplitude and the structure of the SDOS of each spin component have a similar temperature dependence if they are scaled by the transition temperatures,  $T_{c1}$  and  $T_{c2}$ , respectively [24]. However, the magnitudes of the decrease below the kink temperature were quite different as is most easily seen in the temperature dependence of  $Z''$  at the lowest frequency, 9.42 MHz; it was much larger in the  $A_1$  phase than in the  $A_2$  phase. This implies that the exchange of transverse momentum between the wall and the surface

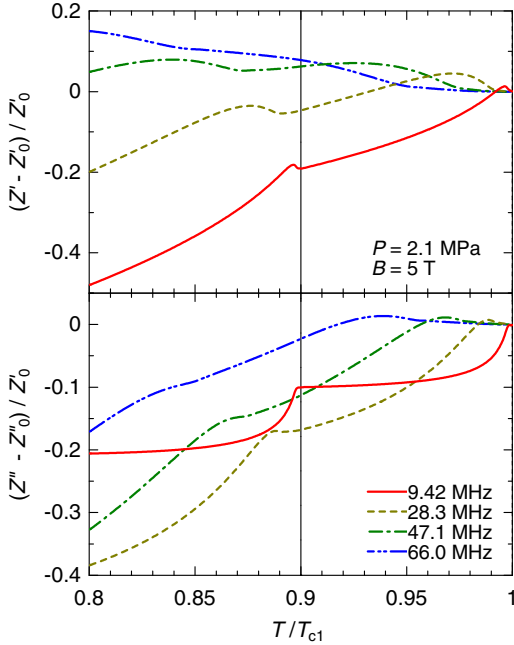


FIG. 2 (color online). Theoretical calculation of the temperature dependence of the real  $Z'$  and imaginary  $Z''$  components of the transverse acoustic impedance at various frequencies. The physical parameters were adjusted to match those of the experiment shown in Fig. 1. Changes from the normal states value  $Z_0$  just above  $T_{c1}$  are plotted. The vertical solid line corresponds to  $T_{c2}$ . Most of the experimental characteristics were reproduced but the temperature dependence of  $Z''$  in the  $A_2$  phase was more significant than that in the experiment.

states was quite different for the two spin components. This point will be revisited in detail later to explore the magnetic field dependence.

The theoretical calculation of the temperature dependence of  $Z$  is shown in Fig. 2. The pressure and magnetic field are the same as those used in the experiment shown in Fig. 1. This calculation procedure has already been reported in Ref. [23]; the order parameters were determined self-consistently on a rough wall and the expectation value of the momentum flux into the wall was estimated by the Keldysh formalism in the weak-coupling approximation to obtain  $Z$ . The effect of the magnetic field was included through the change in  $T_c$ . Magnetic field induced the splitting of  $T_c$  into  $T_{c1}$  and  $T_{c2}$  depending on the spin states and the total acoustic impedance was calculated as a sum of the impedance of each spin component. The Fermi liquid effect was ignored in this calculation. The characteristics exhibited in the experiment were qualitatively reproduced, including the broad peaks in  $Z'$  and the decreases below the kinks in  $Z''$  in both phases, as well as their frequency dependence. The broad peak in  $Z'$  in the  $A_2$  phase is clear in the calculation but is reasonably small to be buried in the experimental noise.

In the calculation, the magnitudes of the decreases below the kink temperature in  $Z''$  were nearly the same in the

$A_1$  and  $A_2$  phases. This is consistent with the naive expectation that the temperature dependence of  $Z$  in the  $A_1$  and  $A_2$  phases is of the same order of magnitude. As shown by the data for 9.42 and 28.3 MHz in Figs. 1 and 2, however, the magnitude of the decrease in the  $A_1$  phase roughly agreed with the experimental result but was significantly larger in the  $A_2$  phase.

In Fig. 3, the temperature dependences of  $Z''$  at a fixed frequency of 28.3 MHz are shown for various magnetic fields up to 13 T at a pressure of 2.8 MPa. The horizontal axis is scaled by  $T_{c1}$  for the corresponding magnetic fields;  $T_{c1}$  increases by about 15% as the magnetic field changes from 0.6 to 13 T.  $T_{c2}$  decreases to  $0.75T_{c1}$  in the highest magnetic field as indicated by the vertical lines.  $Z''$  in the  $A_1$  phase approximately follows a universal curve and decreases to a field independent saturation value  $\delta_{A1}$  at low temperatures. We were able to determine  $\delta_{A1}$  with reasonable accuracy for magnetic fields above 5.0 T but not at 0.6 T where the  $A_1$  phase existed in too narrow a temperature region to reach a saturation value. In higher magnetic fields, the increased  $T_{c1}$  should make the frequency scaled by  $T_{c1}$  effectively lower, but the increase of 15% at most did not have a significant effect on  $Z''$ .

In the  $A_2$  phase, it was difficult to determine the temperature dependence of the spin-down component from the overall values of  $Z''$  because the spin-up component still contributed to the temperature dependence at higher temperatures. At lower temperatures, however,  $Z''$  decreased to a saturation value  $\delta_{A2}$ , which was estimated with good accuracy as shown in Fig. 3. In contrast to the  $A_1$  phase,  $\delta_{A2}$  was weakly dependent on the magnetic field, reducing in

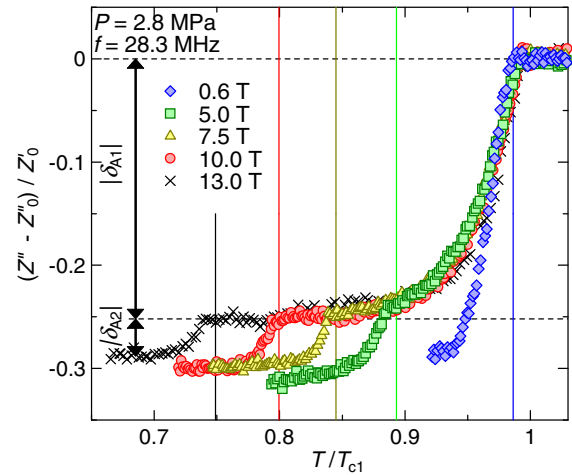


FIG. 3 (color online). Temperature dependence of the imaginary component of the transverse acoustic impedance  $Z''$  under various magnetic fields measured from the normal state value  $Z''_0$ . The temperature was normalized by  $T_{c1}$ . The pressure was 2.8 MPa and the frequency was 28.3 MHz. The vertical lines correspond to  $T_{c2}$  at 0.6, 5.0, 7.5, 10.0, and 13.0 T from right to left. The saturation value in each state,  $\delta_{A1}$  and  $\delta_{A2}$ , was determined as indicated in the figure.



magnitude for higher fields, as was apparent above 5.0 T. As the field increases,  $T_{c2}$  decreases and thus the effective frequency scaled by  $T_{c2}$  should increase. It is reasonable to naively expect that  $Z''$  has a larger temperature dependence at higher effective frequencies. However, this was not observed experimentally and  $\delta_{A2}$  had the opposite dependence.

More unexpectedly,  $|\delta_{A2}|$  was significantly smaller than  $|\delta_{A1}|$ . To see this anomalous behavior clearly, the ratio between  $|\delta_{A1}|$  and  $|\delta_{A2}|$  was plotted against the magnetic field in Fig. 4. Data were plotted for various pressures. It was found that  $|\delta_{A1}|$  was about 5 times larger than  $|\delta_{A2}|$ . The ratio  $|\delta_{A1}|/|\delta_{A2}|$  showed a tendency to be higher in higher magnetic fields as shown in Fig. 4;  $|\delta_{A1}|$  did not depend on the magnetic field but  $|\delta_{A2}|$  became smaller in higher magnetic fields. The solid line is a guide for the eyes.

Measurements at the frequencies of 9.42, 47.1, and 66.0 MHz show a similar difference between  $\delta_{A1}$  and  $\delta_{A2}$  and the magnetic field dependences. However, it was not possible to clearly separate  $\delta_{A1}$  and  $\delta_{A2}$  at high frequencies because the temperature dependence of  $Z''$  was more gradual and did not reach saturation in the  $A_1$  phase.

We also tried to eliminate the effect of thin  $^3\text{He}$  solids adsorbed on the wall by coating the wall with two layers of  $^4\text{He}$ . Although the enhancement of the specularly of the wall was observed as in the superfluid  $B$  phase [17,25,26], the difference between  $\delta_{A1}$  and  $\delta_{A2}$  remained. Thus, the magnetic scattering off the  $^3\text{He}$  solids was shown to be irrelevant to the observed difference in the  $A_1$  and  $A_2$  phases.

In Fig. 4, the dotted line shows the theoretical calculation. In the weak-coupling theory,  $|\delta_{A2}|$  was slightly larger than  $|\delta_{A1}|$  and the ratio  $|\delta_{A1}|/|\delta_{A2}|$  decreased with the magnetic field strength. This is because the frequency is effectively higher in the  $A_2$  phase, which has a lower transition temperature in higher magnetic fields. Therefore,

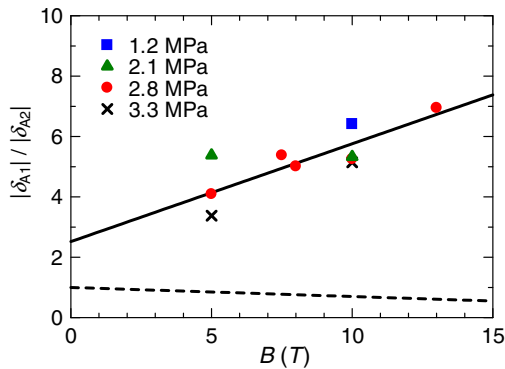


FIG. 4 (color online). Ratio between the saturation values of the transverse acoustic impedance  $Z''$  in the  $A_1$  and  $A_2$  phases  $|\delta_{A1}|/|\delta_{A2}|$  as a function of the magnetic field for several pressures. The frequency was 28.3 MHz. The dotted line shows a simple theoretical calculation. The solid line is a guide for the eyes.

the theoretical calculation of  $|\delta_{A1}|/|\delta_{A2}|$  was about five times smaller than the experimental observation and had the opposite magnetic field dependence. This discrepancy between the experiment and the theory can also be seen in Figs. 1 and 2 as already mentioned.

The large difference between  $\delta_{A1}$  and  $\delta_{A2}$  found experimentally suggests a nonsymmetric acoustic response of the spin-up and spin-down surface states to the transverse oscillation of the wall. This is likely to reflect the intrinsic nature of the nonunitary superfluid phases of  $^3\text{He}$  in very high magnetic fields. One possible origin of the nonsymmetric response is the difference in the coherence length of the spin components. The coherence length is the distance from the wall at which the order parameters are suppressed, and surface states are formed in the suppressed region. The low-lying quasiparticle states of the surface states within the gap energy play a major role in the exchange of transverse momentum with the wall [4,7]. Since the gap amplitudes and transition temperatures can take spin dependent values in nonunitary states, the coherence lengths at zero temperature also depend on the spins as  $\xi_{0\uparrow(\downarrow)} = \hbar v_F / 2\pi k_B T_{c1(2)}$ , and thus  $\xi_{0\downarrow} / \xi_{0\uparrow} > 1$ . Here,  $v_F$  is the Fermi velocity. It is noteworthy that  $\xi_{0\downarrow} / \xi_{0\uparrow}$  is larger in higher magnetic fields, where  $\delta_{A1} / \delta_{A2}$  is larger. The temperature-dependent coherence length is  $\xi_{\uparrow(\downarrow)}(T) = \xi_{0\uparrow(\downarrow)} / (1 - T/T_{c1(2)})^{1/2}$ , and the ratio can be even more enhanced to be  $\xi(T)_{\downarrow} / \xi(T)_{\uparrow} \gg 1$  in the  $A_2$  phase near  $T_{c2}$ .

Although the different coherence lengths were fully taken into account by the self-consistent calculation in Figs. 2 and 4, the coupling between the different spin states was ignored in the weak-coupling approximation and both spin components behaved independently. When mixing mechanisms of the different spin states, i.e., strong-coupling corrections, are properly taken into account, this large difference in coherence lengths may cause the nonsymmetric acoustic response in the  $A_1$  and  $A_2$  phases, although there is no established way of doing this.

Furthermore, to make the different coherence lengths relevant a nonlocal correlation effect has to be included in the calculation of  $Z$ , too. In the presence of a wall that breaks translational symmetry, the Fermi liquid effect induces a coupling between different momentum states that results in a nonlocal correlation in the surface states. Such nonlocal correlation is likely to have a pronounced effect on the exchange of momentum with the wall when the coherence length depends on spin states in nonunitary superfluids. The theory succeeded in describing  $Z$  in the unitary phases as the  $A$  and  $B$  phases [7,9,16]. The theory of  $Z$  would need to be extended to include the strong-coupling corrections and the Fermi liquid effect to quantitatively describe the coupling between nonunitary superfluids and the oscillating wall.

In summary, transverse acoustic impedance was measured in nonunitary  $A_1$  and  $A_2$  phases under very high magnetic fields. Although the energy scale which

characterized the temperature dependence was nearly the same in both phases and the weak-coupling theory reproduced the temperature dependence qualitatively, the magnitude of the temperature dependence was anomalously larger in the  $A_1$  phase than the  $A_2$  phase. This nonsymmetric response implies that the exchange of transverse momentum between the surface states and a wall is dependent on the spin states. Such a spin-dependent process has never been considered theoretically and is possibly a unique feature in nonunitary superfluids.

This study was supported in part by the Global COE Program through the Nanoscience and Quantum Physics Project of Tokyo Tech. and by Grants-in-Aid for Scientific Research (No. 20029009, No. 22340095, and No. 22103003) from MEXT, Japan. This work was carried out as part of the Visiting Researcher's Program of the Institute for Solid State Physics at the University of Tokyo.

---

\*Present address: Cryogenic Research Center, The University of Tokyo, Tokyo 113-0032, Japan.

†Present address: Graduate School of Material Science, University of Hyogo, Hyogo 678-1297, Japan.

‡Present address: Faculty of Education, Gunma University, Maebashi 371-8510, Japan.

- [1] S. Kashiwaya and Y. Tanaka, *Rep. Prog. Phys.* **63**, 1641 (2000).
- [2] L. H. Greene, M. Covington, M. Aprili, E. Badica, and D. E. Pugel, *Physica (Amsterdam)* **280B**, 159 (2000).
- [3] T. Löfwander, V. S. Shumeiko, and G. Wendin, *Supercond. Sci. Technol.* **14**, R53 (2001).
- [4] K. Nagai, Y. Nagato, M. Yamamoto, and S. Higashitani, *J. Phys. Soc. Jpn.* **77**, 111003 (2008).
- [5] A. P. Schnyder, S. Ryu, A. Furusaki, and A. W. W. Ludwig, *Phys. Rev. B* **78**, 195125 (2008).
- [6] A. Kitaev, *AIP Conf. Proc.* **1134**, 22 (2009).
- [7] Y. Okuda and R. Nomura, *J. Phys. Condens. Matter* **24**, 343201 (2012).
- [8] M. Yamamoto, Y. Nagato, S. Higashitani, and K. Nagai, *J. Low Temp. Phys.* **138**, 349 (2005).
- [9] M. Saitoh, Y. Wada, Y. Aoki, S. Murakawa, R. Nomura, and Y. Okuda, *Phys. Rev. B* **74**, 220505 (2006).
- [10] W. P. Halperin and E. Varoquaux, *Helium Three*, edited by W. P. Halperin and L. P. Pitaevskii (North-Holland, Amsterdam, 1990).
- [11] D. Vollhardt and P. Wölfle, *The Superfluid Phases of Helium 3* (Taylor and Francis, London, 1990).
- [12] H. Kojima and H. Ishimoto, *J. Phys. Soc. Jpn.* **77**, 111001 (2008).
- [13] M. Sigrist, *AIP Conf. Proc.* **789**, 165 (2005).
- [14] Y. Nagato, M. Yamamoto, and K. Nagai, *J. Low Temp. Phys.* **110**, 1135 (1998).
- [15] Y. Aoki, Y. Wada, A. Ogino, M. Saitoh, R. Nomura, and Y. Okuda, *J. Low Temp. Phys.* **138**, 783 (2005).
- [16] Y. Aoki, Y. Wada, M. Saitoh, R. Nomura, Y. Okuda, Y. Nagato, M. Yamamoto, S. Higashitani, and K. Nagai, *Phys. Rev. Lett.* **95**, 075301 (2005).
- [17] Y. Wada, S. Murakawa, Y. Tamura, M. Saitoh, Y. Aoki, R. Nomura, and Y. Okuda, *Phys. Rev. B* **78**, 214516 (2008).
- [18] S. Murakawa, Y. Tamura, Y. Wada, M. Wasai, M. Saitoh, Y. Aoki, R. Nomura, Y. Okuda, Y. Nagato, M. Yamamoto, S. Higashitani, and K. Nagai, *Phys. Rev. Lett.* **103**, 155301 (2009).
- [19] S. Murakawa, Y. Wada, Y. Tamura, M. Wasai, M. Saitoh, Y. Aoki, R. Nomura, Y. Okuda, Y. Nagato, M. Yamamoto, S. Higashitani, and K. Nagai, *J. Phys. Soc. Jpn.* **80**, 013602 (2011).
- [20] L. P. Roobol, P. Remeijer, S. C. Steel, R. Jochemsen, V. S. Shumeiko, and G. Frossati, *Phys. Rev. Lett.* **79**, 685 (1997).
- [21] D. C. Sagan, P. G. N. deVegvar, E. Polturak, L. Friedman, S. -S. Yan, E. L. Ziercher, and D. M. Lee, *Phys. Rev. Lett.* **53**, 1939 (1984).
- [22] U. E. Israelsson, B. C. Crooker, H. M. Bozler, and C. M. Gould, *Phys. Rev. Lett.* **53**, 1943 (1984).
- [23] Y. Nagato, M. Yamamoto, S. Higashitani, and K. Nagai, *J. Low Temp. Phys.* **149**, 294 (2007).
- [24] S. Murakawa, A. Yamaguchi, M. Arai, M. Wasai, Y. Aoki, H. Ishimoto, R. Nomura, and Y. Okuda, *J. Low Temp. Phys.* **158**, 141 (2010).
- [25] Y. Tamura, S. Murakawa, Y. Wada, M. Wasai, M. Saitoh, Y. Aoki, R. Nomura, and Y. Okuda, *J. Phys. Conf. Ser.* **150**, 032106 (2009).
- [26] S. Murakawa, M. Wasai, K. Akiyama, Y. Wada, Y. Tamura, R. Nomura, and Y. Okuda, *Phys. Rev. Lett.* **108**, 025302 (2012).